LINK INVARIANTS VIA COUNTING SURFACES

MICHAEL BRANDENBURSKY

Abstract. A Gauss diagram is a simple, combinatorial way to present a knot. It is known that any Vassiliev invariant may be obtained from a Gauss diagram formula that involves counting (with signs and multiplicities) subdiagrams of certain combinatorial types. These formulas generalize the calculation of a linking number by counting signs of crossings in a link diagram. Until recently, explicit formulas of this type were known only for few invariants of low degrees. In this paper we present simple formulas for an infinite family of invariants in terms of counting surfaces of a certain genus and number of boundary components in a Gauss diagram. We then identify the resulting invariants with certain derivatives of the HOMFLYPT polynomial.

1. Introduction.

In this paper we consider link invariants arising from the Conway and HOMFLYPT polynomials. The HOMFLYPT polynomial $P(L)$ is an invariant of an oriented link L (see e.g. [9], [16], [21]). It is a Laurent polynomial in two variables a and z, which satisfies the following skein relation:

(1) $$aP\left(\quad\right) - a^{-1}P\left(\quad\right) = zP\left(\quad\right).$$

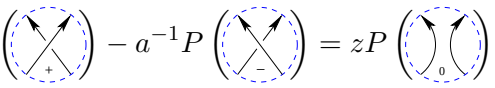

The HOMFLYPT polynomial is normalized in the following way. If O_m is an m-component unlink, then $P(O_m) = \left(\frac{a-a^{-1}}{z}\right)^{m-1}$. The Conway polynomial ∇ may be defined as $\nabla(L) := P(L)|_{a=1}$. This polynomial is a renormalized version of the Alexander polynomial (see e.g. [7], [15]). All coefficients of ∇ are finite type or Vassiliev invariants.

One of the mainstream and simplest techniques for producing Vassiliev invariants are so-called Gauss diagram formulas (see [10], [20]). These formulas generalize the calculation of a linking number by counting subdiagrams of special geometric-combinatorial types with signs and weights in a given link diagram. This technique is also very helpful in the rapidly developing field of virtual knot theory (see [12]), as well as in 3-manifold theory (see [17]).

Until recently, explicit formulas of this type were known only for few invariants of low degrees. The situation has changed with works of Chmutov-Khoury-Rossi [3] and Chmutov-Polyak [5], see also [14] for the case of string links. In [3] Chmutov-Khoury-Rossi presented an infinite family of Gauss diagram formulas for all coefficients of $\nabla(L)$, where L is a knot or a two-component link. We explain how each formula for the coefficient c_n of z^n is related to a certain count of orientable surfaces of a

certain genus, and with one boundary component. The genus depends only on n and the number of the components of L. These formulas may be viewed as a certain combinatorial analog of Gromov-Witten invariants.

In this work we generalize the result of Chmutov-Khoury-Rossi to links with arbitrary number of components. We present a direct proof of this result, without any prior assumption on the existence of the Conway polynomial. It enables us to present two different extensions of the Conway polynomial to long virtual links. We compare these extensions with the existing versions of the Alexander and Conway polynomials for virtual links, and show that they are new. In particular, we give a new proof of the fact that the famous Kishino knot K_T [13] is non-classical, by calculating these polynomials for K_T. Later we show that these formulas may be modified by counting only certain, so-called irreducible, subdiagrams.

This leads to a natural question: how to produce link invariants by counting orientable surfaces with an arbitrary number of boundary components? In this paper we deal with a model case, when the number of boundary components is two. We modify Chmutov-Khoury-Rossi construction and present an infinite family of Gauss diagram formulas for the coefficients of the first partial derivative of the HOMFLYPT polynomial, w.r.t. the variable a, evaluated at $a = 1$. This family is related, in a similar way, to the family of orientable surfaces with two boundary components. Later we modify these formulas in case of knots.

In the forthcoming paper [2] we show that, in case of closed braids, a similar count of orientable surfaces with n boundary components (up to some normalization) is related to an infinite family of Gauss diagram formulas for the coefficients of the $n-1$ derivative, w.r.t. the variable a in the HOMFLYPT polynomial, evaluated at $a = 1$.

Acknowledgments. I would like to thank Michael Polyak, who has introduced me to this subject, guided and helped me a lot while I was working on this paper. I also would like to thank the referee for careful reading of this paper and for his/her useful comments and remarks.

Part of this work has been done during the author's stay at Max Planck Institute for Mathematics in Bonn. The author wishes to express his gratitude to the Institute for the support and excellent working conditions.

2. Gauss diagrams and arrow diagrams

In this section we recall a notion of Gauss diagrams, arrow diagrams and Gauss diagram formulas. We then define a special type of arrow diagrams which will be used to define Gauss diagram formulas for coefficients of the Conway polynomial, and for coefficients of some other polynomials derived from the HOMFLYPT polynomial.

2.1. Gauss diagrams of classical and virtual links.

Gauss diagrams (see e.g. [8], [10], [20]) provide a simple combinatorial way to encode classical and virtual links.

Definition 2.1. Given a classical (possibly framed) link diagram D, consider a collection of oriented circles parameterizing it. Unite two preimages of every crossing of D in a pair and connect them by an arrow, pointing from the overpassing preimage to

the underpassing one. To each arrow we assign a sign (writhe) of the corresponding crossing. The result is called the *Gauss diagram* G corresponding to D.

We consider Gauss diagrams up to an orientation-preserving diffeomorphisms of the circles. In figures we will always draw circles of the Gauss diagram with a counterclockwise orientation.

Example 2.2. Diagrams of the trefoil knot and the Hopf link, together with the corresponding Gauss diagrams, are shown in the following picture.

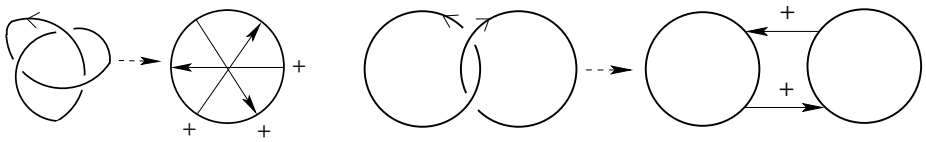

A classical link can be uniquely reconstructed from the corresponding Gauss diagram [10]. Many fundamental knot invariants, such as the knot group and the Alexander polynomial, may be easily obtained from the Gauss diagram. We are going to work with *based Gauss diagrams*, i.e. Gauss diagrams with a base point (different from the endpoints of the arrows) on one of the circles. If we cut a based circle at the base point, we will get a Gauss diagram of a long link, see Figure 1.

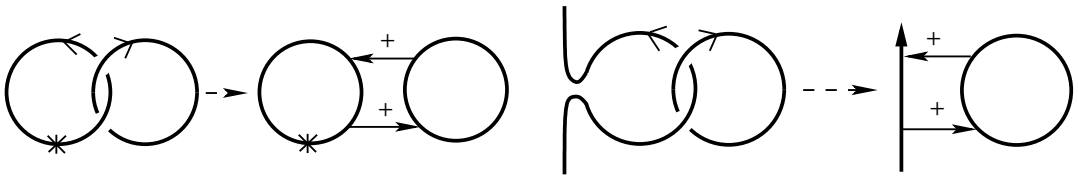

FIGURE 1. Diagrams of based and long classical Hopf links together with the associated Gauss diagrams.

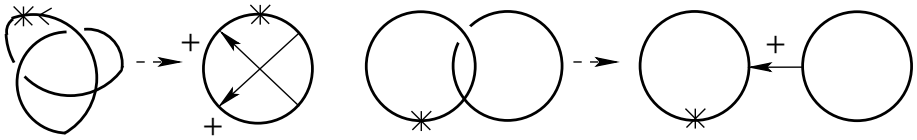

FIGURE 2. Virtual trefoil and a virtual Hopf link with the corresponding Gauss diagrams.

Note that not every collection of circles with signed arrows is realizable as a Gauss diagram of a classical link, see Figure 2. The Gauss diagram of a virtual link diagram is constructed in the same way as for a classical link diagram, but all virtual crossings are disregarded, see Figure 2. Similarly to the case of long classical links, each non-realizable Gauss diagram with a base point represents a long virtual link.

Two Gauss diagrams represent isotopic classical/virtual links (long links) if and only if they are related by a finite number of Reidemeister moves for Gauss diagrams (applied away from the base point) shown in Figure 3, where $\varepsilon = \pm 1$, see e.g. [4, 18, 19]. Note that not all Reidemeister moves are shown in Figure 3 (for example third Reidemeister moves with at least one negative crossing are not shown), but their generating set is, see [19].

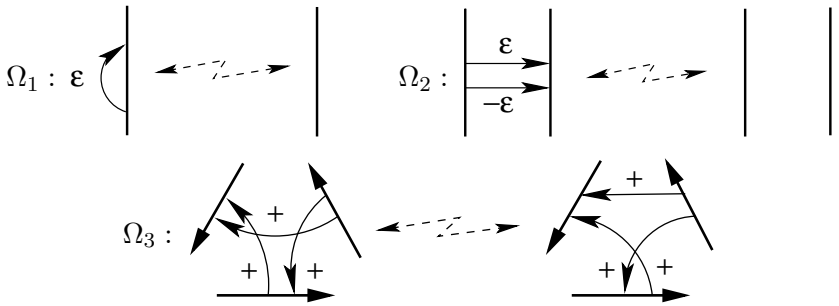

FIGURE 3. Reidemeister moves of Gauss diagrams.

Two Gauss diagrams represent isotopic classical framed links if and only if they are related by a finite number of Reidemeister moves for framed Gauss diagrams. It suffices to consider Ω_2 and Ω_3 of Figure 3 and substitute the move Ω_1 by the move

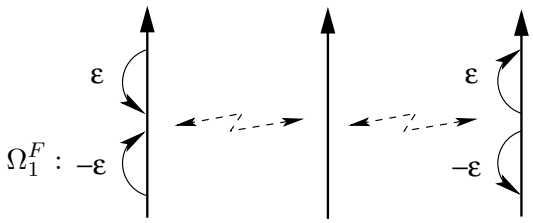

Note that segments involved in Ω_2 or Ω_3 may lie on different components of the link and the order in which they are traced along the link may be arbitrary.

2.2. **Arrow diagrams and Gauss diagram formulas.** An *arrow diagram* is a modification of a notion of a Gauss diagram, in which we forget about realizability and signs of arrows, see Figure 4.

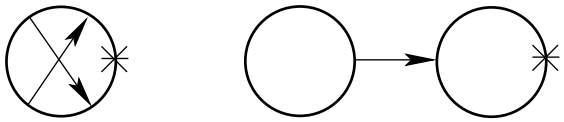

FIGURE 4. Connected arrow diagrams.

In other words, an arrow diagram consists of a number of oriented circles with several arrows connecting pairs of distinct points on them. We consider these diagrams up to orientation-preserving diffeomorphisms of the circles. An arrow diagram is *based*, if a base point (different from the end points of the arrows) is marked on one of the circles. An arrow diagram is connected, if it is connected as a graph. Further we will consider only based connected arrow diagrams, so we will omit mentioning these requirements throughout this chapter, unless a misunderstanding is likely to occur. In figures we will always draw the circles of an arrow diagram with a counter-clockwise orientation.

M. Polyak and O. Viro suggested [20] the following approach to compute link invariants using Gauss diagrams.

Definition 2.3. Let A be an arrow diagram with m circles and let G be a based Gauss diagram of an m-component oriented (long, virtual) link. A *homomorphism* $\phi : A \to G$ is an orientation preserving homeomorphism between each circle of A and each circle of G, which maps a base point of A to the base point of G and induces an injective map of arrows of A to the arrows of G. The set of arrows in $\mathrm{Im}(\phi)$ is called a *state* of G induced by ϕ and is denoted by $S(\phi)$. The *sign* of ϕ is defined as $\mathrm{sign}(\phi) = \prod_{\alpha \in S(\phi)} sign(\alpha)$. A set of all homomorphisms $\phi : A \to G$ is denoted by $\mathrm{Hom}(A, G)$.

Note that since the circles of A are mapped to circles of G, a state S of G determines both the arrow diagram A and the map $\phi : A \to G$ with $S = S(\phi)$.

Definition 2.4. A *pairing* between an arrow diagram A and G is defined by

$$\langle A, G \rangle = \sum_{\phi \in \mathrm{Hom}(A,G)} \mathrm{sign}(\phi).$$

For an arbitrary arrow diagram A the pairing $\langle A, G \rangle$ does not represent a link invariant, i.e. it depends on the choice of a Gauss diagram of a link. However, for some special linear combinations of arrow diagrams the result is independent of the choice of G, i.e. does not change under the Reidemeister moves for Gauss diagrams. Using a slightly modified definition of arrow diagrams Goussarov, Polyak and Viro showed in [10] that each real-valued Vassiliev invariant of long knots may be obtained this way. In particular, all coefficients of the Conway polynomial may be obtained using suitable combinations of arrow diagrams.

2.3. **Surfaces corresponding to arrow diagrams.** Given an arrow diagram A, we define an oriented surface $\Sigma(A)$ as follows. Firstly, replace each circle of A with an oriented disk bounding this circle. Secondly, glue 1-handles to boundaries of these disks using each arrow as a core of a ribbon. See Figure 5.

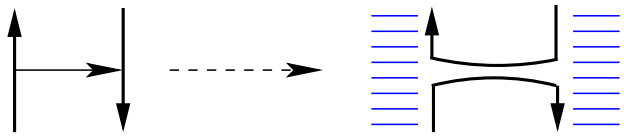

FIGURE 5. Constructing a surface from an arrow diagram.

Definition 2.5. By the *genus* and the *number of boundary components* of an arrow diagram A we mean the genus and the number of boundary components of $\Sigma(A)$.

Remark 2.6. Let A be an arrow diagram with n arrows and m circles. Then the Euler characteristic χ of $\Sigma(A)$ equals to $\chi(\Sigma(A)) = m - n$. If A is connected, $n \geq m - 1$. If A has one boundary component, $n \neq m (\mathrm{mod} 2)$.

Example 2.7. The arrow diagram with one circle in Figure 4 is of genus one, while the other arrow diagram in the same figure is of genus zero. Both of them have one boundary component.

Further we will work only with based connected arrow diagrams with one or two boundary components.

2.4. **Ascending and descending arrow diagrams.** In this subsection we define a special type of arrow diagrams with one and two boundary components.

Definition 2.8. Let A be a based arrow diagram with one boundary component. As we go along the boundary of $\Sigma(A)$ starting from the base point, we pass on the boundary of each ribbon twice: once in the direction of its core arrow, and once in the opposite direction. A is *ascending* (respectively, *descending*) if we pass each ribbon of $\Sigma(A)$ first time in the direction opposite to its core arrow (respectively, in the direction of its core arrow).

Remark 2.9. In order to define the notion of ascending and descending arrow diagrams we used the fact that all arrow diagrams are based and connected. The position of the base point in a connected arrow diagram is essential to define an order of passage.

Example 2.10. Arrow diagrams presented below are ascending (a), descending (b) and neither ascending nor descending (c).

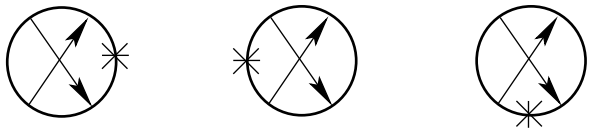

Denote by $\mathcal{A}_{n,m}$ (respectively, $\mathcal{D}_{n,m}$) the set of all ascending (respectively, descending) arrow diagrams with n arrows, m circles and one boundary component.

Example 2.11. The sets $\mathcal{A}_{2,1}$ and $\mathcal{D}_{2,1}$ are presented below.

$\mathcal{A}_{2,1} :=$  and $\mathcal{D}_{2,1} :=$ 

Definition 2.12. Let G be any Gauss diagram with m circles. We set

$$A_{n,m}(G) := \sum_{A\in\mathcal{A}_{n,m}} \langle A, G\rangle \qquad D_{n,m}(G) := \sum_{A\in\mathcal{D}_{n,m}} \langle A, G\rangle$$

and define the following polynomials:

$$\nabla_{asc}(G) := \sum_{n=0}^{\infty} A_{n,m}(G)z^n \qquad \nabla_{des}(G) := \sum_{n=0}^{\infty} D_{n,m}(G)z^n$$

These polynomials will play an important role in the next section. Now we generalize a notion of ascending (descending) arrow diagram to arrow diagrams with two boundary components. We would like to point out that in [2] this notion is generalized for arrow diagrams with arbitrary number of boundary components.

Definition 2.13. Let A be an arrow diagram with two boundary components. As we go along the component of $\partial\Sigma(A)$ starting from the base point, we pass on the boundary of each ribbon once or twice (since A is connected we must pass all ribbons at least once). We call core arrows, which we pass only in one direction, the *separating arrows*. Now we place another starting point $\bullet$ on the second component of $\partial\Sigma(A)$ near the first separating arrow which we encounter in the passage, and start going

along this component of $\partial\Sigma(A)$. A is *ascending* (respectively, *descending*) if we pass each ribbon of $\Sigma(A)$ first time in the direction opposite to its core arrow (respectively, in the direction).

Example 2.14. Arrow diagrams below have two boundary components. Diagram (a) is ascending and diagram (b) is descending. Separating arrows are shown in bold.

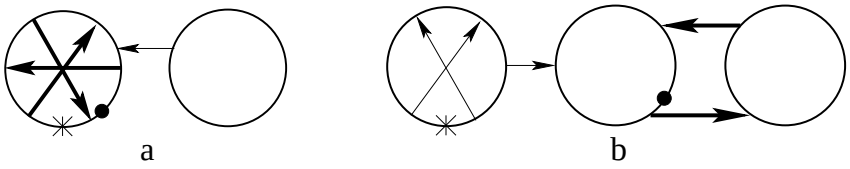

Denote by $\mathcal{A}^2_{n,m}$ (respectively, $\mathcal{D}^2_{n,m}$) the set of all ascending (respectively, descending) arrow diagrams with n arrows, m circles and two boundary components.

Example 2.15. All diagrams in the set $\mathcal{A}^2_{2,2}$ are presented below.

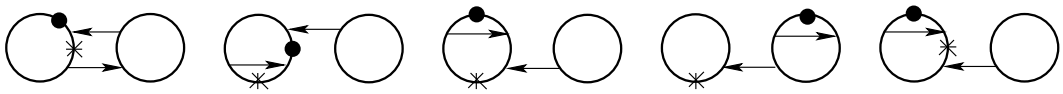

Let G be any Gauss diagram with m circles. We set

$$A^2_{n,m}(G) := \sum_{A\in\mathcal{A}^2_{n,m}} \langle A, G\rangle \qquad D^2_{n,m}(G) := \sum_{A\in\mathcal{D}^2_{n,m}} \langle A, G\rangle.$$

A state $S(\phi)$ corresponding to $\phi : A \to G$ for an ascending (respectively descending) diagram A with one or two boundary components will be also called *ascending* (respectively *descending*). It is useful to reformulate this notion in terms of a tracing of a diagram G.

Definition 2.16. Given $\phi : A \to G$, a passage along the boundary of the surface $\Sigma(A)$ induces a *tracing* of G: we follow an arc of a circle of G starting from the base point until we hit an arrow in $S(\phi)$, turn to this arrow, then continue on another arc of G following the orientation and so on, until we return to the base point. In case of two boundary components we repeat the same procedure starting near the image of the first separating arrow. Then a state $S(\phi)$ is *ascending* (respectively *descending*), if we approach every arrow in the tracing first time at its head (respectively at its tail).

2.5. **Separating states.** In this subsection we define a notion of a separating state. This notion will be extensively used in the following sections.

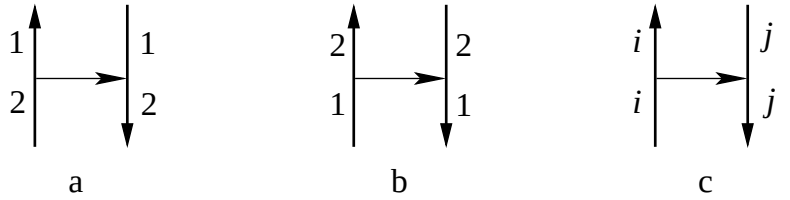

FIGURE 6. Ascending and descending labeling. Here $i, j \in \{1, 2\}$.

Definition 2.17. Let G be a based Gauss diagram. An *ascending (respectively descending) separating state S of G* is a state S of G, together with a labeling of arcs of G (i.e., intervals of circles of G between endpoints of arrows) by 1 and 2 such that:

(1) Each arc near $\alpha \in S$ is labeled as in Figure 6a (respectively in Figure 6b).

(2) Each arc near $\alpha \notin S$ is labeled as in Figure 6c.

(3) An arc with a base point is labeled by 1.

Every separating (ascending or descending) state S in G defines a new Gauss diagram G_S with labeled circles as follows: We smooth each arrow in G which belongs to S, see Figure 7, and denote the resulting smoothed Gauss diagram by G_S. Each circle in G_S is labeled by i, if it contains an arc labeled by i.

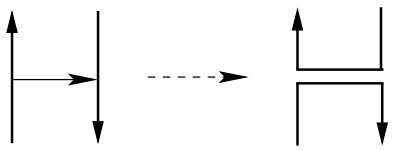

FIGURE 7. Smoothing of an arrow.

Now we return to arrow diagrams with two boundary components. Let $A \in \mathcal{A}^2_{n,m}$ or $A \in \mathcal{D}^2_{n,m}$. We denote by $\sigma(A)$ the set of separating arrows in A and label the arcs of circles in A by 1 if the corresponding arc belongs to the first boundary component of $\Sigma(A)$ and by 2 otherwise.

Note that each homomorphism $\phi : A \to G$ induces an ascending or descending separating state S of G, by taking $S = \phi(\sigma(A))$ and labeling each arc of G by the same label as the corresponding arc of A.

Definition 2.18. Let G be a based Gauss diagram with m circles. Let S be an ascending (respectively descending) separating state of G, $A \in \mathcal{A}^2_{n,m}$ (respectively $A \in \mathcal{D}^2_{n,m}$), and $\phi : A \to G$. We say that ϕ is *S-admissible*, if an ascending (respectively descending) separating state induced by ϕ coincides with S.

Definition 2.19. Let S be an ascending (respectively descending) separating state of G, and $A \in \mathcal{A}^2_{n,m}$ (respectively $A \in \mathcal{D}^2_{n,m}$). In each case we define an *S-pairing* $\langle A, G\rangle_S$ by:

$$\langle A, G\rangle_S := \sum_{\phi: A\to G} \mathrm{sign}(\phi),$$

where the summation is over all S-admissible $\phi : A \to G$. We set

$$A^2_{n,m}(G)_S := \sum_{A\in\mathcal{A}^2_{n,m}} \langle A, G\rangle_S \quad \text{and} \quad D^2_{n,m}(G)_S := \sum_{A\in\mathcal{D}^2_{n,m}} \langle A, G\rangle_S.$$

3. Counting surfaces with one boundary component

In this section we review Gauss diagram formulas for coefficients of the Conway polynomial ∇ obtained in [3, Theorem 3.5] for classical knots and 2-component classical links.

Theorem 3.1 ([3]). *Let G be a Gauss diagram of a classical knot or 2-component classical link L.*

$$\nabla_{asc}(G) = \nabla_{des}(G) = \nabla(L), \tag{2}$$

where $\nabla(L)$ is the Conway polynomial.

Let G be a Gauss diagram with m circles. We give a direct proof of the invariance of both $\nabla_{asc}(G)$ and $\nabla_{des}(G)$ under the Reidemeister moves which do not involve a base point. This allows us to extend this result to m-component classical links and also to define two different generalizations of the Conway polynomial to long virtual links. At the end of this section we present some properties of these polynomials.

3.1. **Invariants of long links.** In this subsection we generalize the result of [3] to m-component (classical or virtual) long links.

Theorem 3.2. *Let G be a Gauss diagram of an m-component (classical or virtual) long link L. Then $\nabla_{asc}(G)$ and $\nabla_{des}(G)$ define polynomial invariants of long links, i.e. do not depend on the choice of G.*

Proof. We prove that $\nabla_{asc}(G)$ is an invariant of an underlying link. The proof for $\nabla_{des}(G)$ is the same. It suffices to show that $A_{n,m}(G)$ is invariant under the Reidemeister moves Ω_1, Ω_2 and Ω_3 of Figure 3 applied away from the base point. Let G and $\widetilde{G}$ be two Gauss diagrams that differ by an application of Ω_1, so that $\widetilde{G}$ has one additional isolated arrow α on one of the circles. Ascending states of G are in bijective correspondence with ascending states of $\widetilde{G}$ which do not contain α. But α cannot not be in the image of $\phi : A \to \widetilde{G}$ with $A \in \mathcal{A}_{n,m}$, because A should have one boundary component. Thus $A_{n,m}(G) = A_{n,m}(\widetilde{G})$.

Let G and $\widetilde{G}$ be two Gauss diagrams that differ by an application of Ω_2, so that $\widetilde{G}$ has two additional arrows α_ε and $\alpha_{-\varepsilon}$, see Figure 3. Ascending states of G are in bijective correspondence with ascending states of $\widetilde{G}$ which do not contain $\alpha_{\pm\varepsilon}$. Note that both α_ε and $\alpha_{-\varepsilon}$ can not be in the image of $\phi : A \to \widetilde{G}$ with $A \in \mathcal{A}_{n,m}$ because A has one boundary component. Ascending states of $\widetilde{G}$ which contain one of $\alpha_{\pm\varepsilon}$ come in pairs $S \cup \alpha_\varepsilon$ and $S \cup \alpha_{-\varepsilon}$ with opposite signs, thus cancel out in $A_{n,m}(\widetilde{G})$. Hence

$$A_{n,m}(G) = A_{n,m}(\widetilde{G}).$$

Let G and $\widetilde{G}$ be two Gauss diagrams that differ by an application of Ω_3, as shown in Figure 3 (G is on the left and $\widetilde{G}$ is on the right).

Then there is a bijective correspondence between ascending states of G and $\widetilde{G}$. This correspondence preserves the signs and the combinatorics of the order in which the tracing enters and leaves the neighborhood of these arrows. The table below summarizes this correspondence.

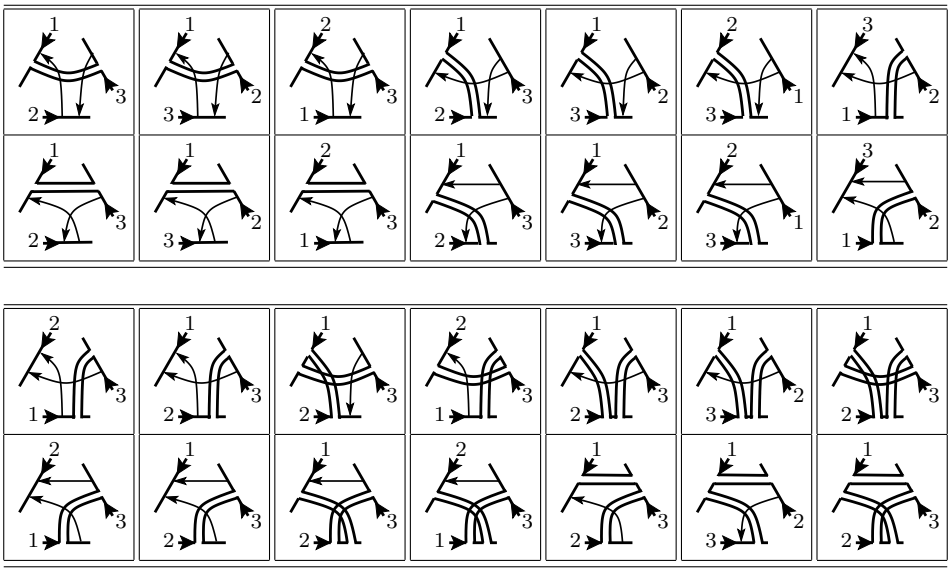

For a better understanding of this table, let us explain one of the cases in details. Denote the top, left, and right arrows in the fragment by α_t, α_l, and α_r respectively.

Consider a state $S \cup \alpha_l \cup \alpha_r$ of G which contains two arrows of the fragment. The order of tracing the fragment depends on S. Only two orders of tracing may give an ascending state:

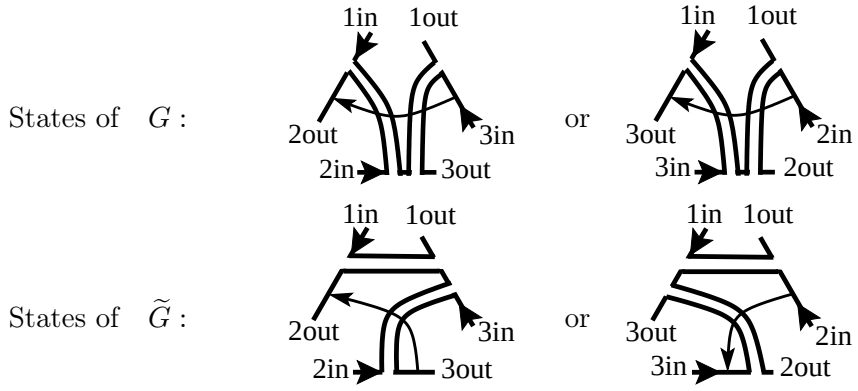

Here the three consecutive entries and exits from the fragment are indicated by 1in, 1out, 2in, 2out, 3in, 3out. In the first case, the corresponding state of $\widetilde{G}$ is $S \cup \alpha_t \cup \alpha_r$. Note that the pattern of entries and exits from the fragment is indeed the same as in G. In the second case, the corresponding state of $\widetilde{G}$ is $S \cup \alpha_t \cup \alpha_l$. The pattern of entries and exits is again the same as in G. □

3.2. **Properties of $A_{n,m}(G)$ and $D_{n,m}(G)$.**

Theorem 3.3. *Let G_+, G_- and G_0 be Gauss diagrams which differ only in the fragment shown in Figure 8. Then*

$$(3) \quad \nabla_{asc}(G_+) - \nabla_{asc}(G_-) = z\nabla_{asc}(G_0) \qquad \nabla_{des}(G_+) - \nabla_{des}(G_-) = z\nabla_{des}(G_0).$$

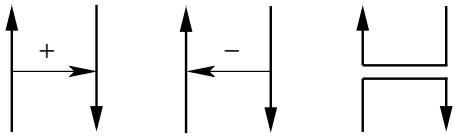

FIGURE 8. A Conway triple of Gauss diagrams.

Proof. Again we will prove this theorem for ∇_{asc}. Denote by m and m_0 the number of circles in $G_\pm$ and G_0, respectively. It is enough to prove that for each n we have

$$A_{n,m}(G_+) - A_{n,m}(G_-) = A_{n-1,m_0}(G_0). \tag{4}$$

Denote the arrows of G_+ and G_- appearing in the fragment in Figure 8 by α_+ and α_-, respectively. The proof of the skein relation is the same as in [3]. All ascending states of $G_\pm$ which do not contain $\alpha_\pm$ cancel out in (4) in pairs. Each ascending state $S \cup \alpha_\pm$ of $G_\pm$ corresponds to a unique ascending state S of G_0, and vice versa: if S is an ascending state of G_0, then (depending on the order of the fragments in the tracing) exactly one of $S \cup \alpha_+$ and $S \cup \alpha_-$ will give an ascending state on either G_+ or G_-. □

It is easy to see that both $A_{n,m}(G)$ and $D_{n,m}(G)$ depend on the position of the base point when G is a Gauss diagram associated with a virtual link diagram. Let G and $\widehat{G}$ be two Gauss diagrams shown in Figure 9. Then $A_{2,1}(G) = 1$, $A_{2,1}(\widehat{G}) = 0$, $D_{2,1}(G) = 0$, $D_{2,1}(\widehat{G}) = 1$.

However, for classical links this is not the case. Our next theorem states that in the case of classical links, both $\nabla_{asc}(G)$ and $\nabla_{des}(G)$ are independent of the position of the base point.

FIGURE 9. Dependence on a basepoint.

Theorem 3.4. *Let G be a based Gauss diagram of an m-component classical link L. Both $\nabla_{asc}(G)$ and $\nabla_{des}(G)$ are independent of the position of the base point.*

Proof. We will prove the independence of $A_{n,m}(G)$ of the position of the base point, the proof for $D_{n,m}(G)$ is the same. We prove this statement by induction on the number of arrows in G.

If G has no arrows, there is nothing to prove. Now let us assume that the statement holds for any (classical) Gauss diagram with less than k arrows, and let G be a Gauss diagram with k arrows. If $k < n$, then $A_{n,m}(G) = 0$ and we are done, so we may assume that $k \geq n$. Suppose that the base point lies on the i-th component of G. We should prove that we may move the base point across any arrowhead or arrowtail

on the i-th component, and to shift it to any other, say, j-th, component. Denote by $G_1, \ldots, G_7$ Gauss diagrams which differ only in a fragment which looks like

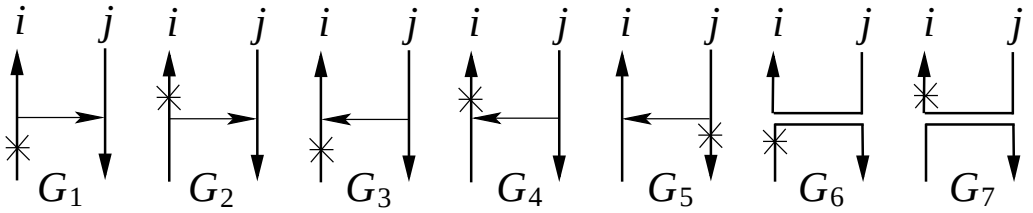

respectively. It suffices to prove that we have:

$$A_{n,m}(G_1) = A_{n,m}(G_2)\ ,\ \ A_{n,m}(G_3) = A_{n,m}(G_4)\ ,\ \ A_{n,m}(G_3) = A_{n,m}(G_5). \tag{5}$$

Denote by α the arrow appearing in the fragment above. The first equality is immediate; indeed, in G_1 and G_2 there are no ascending states with one boundary component which contain α (and all other ascending states are in a bijective correspondence).

To prove the second equation in (5), note that there is a bijection between ascending states of $A_{n,m}(G_3)$ and $A_{n,m}(G_4)$ which do not contain α; the remaining ascending states of G_3 and G_4 look exactly like the ones of G_6 and G_7, respectively; thus we have

$$A_{n,m}(G_3) - A_{n,m}(G_4) = A_{n-1,m_0}(G_6) - A_{n-1,m_0}(G_7) = 0,$$

where $m_0 = m \pm 1$ is the number of circles in G_6 and G_7 and the second equality holds by the induction hypothesis. It is worth to mention that since G_3 and G_4 are diagrams of classical links, then so are G_6 and G_7.

The proof of the last equality in (5) is more complicated. We will use an inner induction on the number r of arrows which have only their arrowtail on the i-th component. If $r = 0$, then $A_{n,m}(G_3) = A_{n,m}(G_5) = 0$. Indeed, for $r = 0$ there are no ascending states in G_5 (since we cannot reach the i-th circle), so $A_{n,m}(G_5) = 0$. Also, since $r = 0$, i-th component of the link is under all other components, so we may move it apart by a finite sequence of Reidemeister moves Ω_2 and Ω_3 applied away from the base point, converting G_3 into a Gauss diagram with an isolated i-th component (here we use the fact that G_3 is associated with a classical link diagram); thus $A_{n,m}(G_3) = 0$ by Theorem 3.2.

Let's establish the step of induction. On both G_3 and G_5 pick the same arrow, which has only its arrowtail on the i-th component, and apply the skein relation of Theorem 3.3 to simplify the corresponding Gauss diagrams. Diagrams on the right-hand side of the skein relation have less than k crossings, so the right-hand sides are equal by the induction on k; the remaining terms in the left-hand side are also equal by induction on r. □

Corollary 3.5. *Let G be a Gauss diagram of an m-component classical link L. Then*

$$\nabla_{asc}(G) = \nabla_{des}(G) = \nabla(L),$$

i.e. for every n we have $A_{n,m}(G) = D_{n,m}(G) = c_n(L)$.

Proof. By Theorems 3.2 – 3.4, $A_{n,m}(G)$ and $D_{n,m}(G)$ are link invariants which satisfy the same skein relation as $c_n(L)$. It remains to compare their normalization, i.e. their

values on the unknot O. A standard Gauss diagram $G(O)$ of an unknot consists of one circle with no arrows. It follows that $D_{0,1}(G(O)) = A_{0,1}(G(O)) = 1$, and $D_{n,m}(G(O)) = A_{n,m}(G(O)) = 0$ otherwise. Hence $A_{n,m}(G)$ and $D_{n,m}(G)$ have the same normalization as $c_n(L)$ and the corollary follows. □

Example 3.6. Consider a 3-component link L and the Gauss diagram G of L shown below:

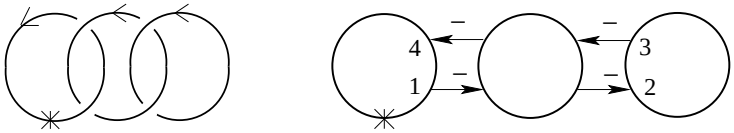

The only ascending state of G is $\{3, 4\}$. It sign is $+$. Thus $c_2(L) = 1$ and $c_n(L) = 0$ for all $n \neq 2$, so $\nabla(L) = z^2$.

3.3. **Alexander-Conway polynomials of long virtual links.** In this subsection we study properties of the polynomials ∇_{asc} and ∇_{des} for long virtual links, and compare them with other existing constructions.

Let L be a classical or long virtual link and G be any Gauss diagram of L. Polynomials $\nabla_{asc}(L) := \nabla_{asc}(G)$ and $\nabla_{des}(L) := \nabla_{des}(G)$ were defined in [3], but the proof that they are well defined for classical links with more than 2 components and for long virtual links was not presented. By Theorem 3.2 and Corollary 3.5, $\nabla_{asc}(L)$ and $\nabla_{des}(L)$ are invariants of L, and if L is a classical link

$$\nabla_{asc}(L) = \nabla_{des}(L) = \nabla(L).$$

Note that for long virtual links it may happen that

$$\nabla_{asc}(L) \neq \nabla_{des}(L).$$

For example, let G be a Gauss diagram of the long virtual Hopf link L shown in Figure 2. Then $\nabla_{asc}(L) = z$, but $\nabla_{des}(L) = 0$. We denote by

$$\nabla_{asc-des}(L) := \nabla_{asc}(L) - \nabla_{des}(L).$$

This polynomial vanishes on classical links but, as we will see below, may be used to distinguish virtual links from classical links.

Let D be a diagram of a (long) virtual link L and G its corresponding Gauss diagram. Pick a classical crossing on D. A move on D and the corresponding move on G shown in Figure 10 is called the *virtualization* move.

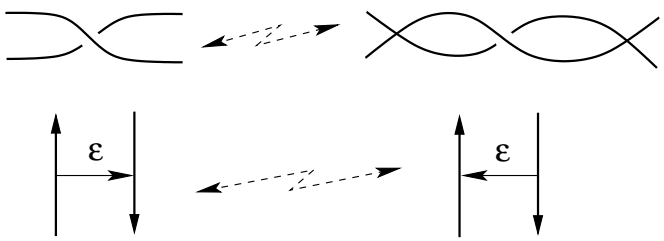

FIGURE 10. The virtualization move.

Theorem 3.7. *Let L and L_1 be long virtual links. Then the following holds.*

(1) $\nabla_{asc}(L\#L_1) = \nabla_{asc}(L)\nabla_{asc}(L_1)$, $\nabla_{des}(L\#L_1) = \nabla_{des}(L)\nabla_{des}(L_1)$, *where* $L\#L_1$ *denotes a long virtual link which is a connected sum of* L *and* L_1.

(2) *Non-trivial coefficients of* ∇_{des} *and* ∇_{asc} *are not invariant under the virtualization move*

(3) *Coefficients of* $\nabla_{des}(L)$ *and* $\nabla_{asc}(L)$ *are Vassiliev invariants in the sense of both GPV* [10] *and Kauffman* [12].

Proof. The proof of (1) is straightforward and follows from the definition of ∇_{asc} and ∇_{des}.

Now we prove (2). Consider even n first. Let $n = 2k$ and let G and G_1 be Gauss diagrams of long virtual knots shown in Figure 11a and 11b respectively. Note that G and G_1 differ by an application of the virtualization move. Both G and G_1 have $n+1$ arrows. It is easy to check that

$$A_{n,1}(G) = -1 \quad D_{n,1}(G) = 1, \quad \text{but} \quad A_{n,1}(G_1) = D_{n,1}(G_1) = 0.$$

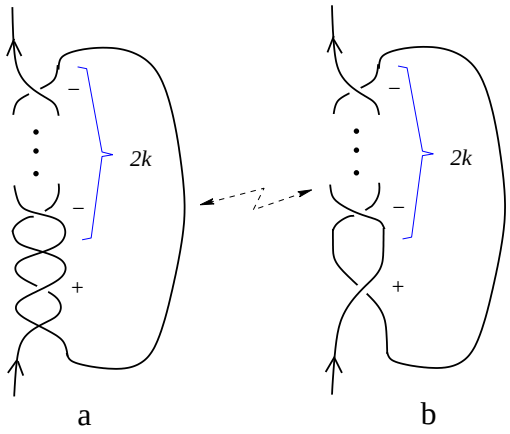

FIGURE 11. Diagrams of long virtual knots that differ by an application of the virtualization move.

To prove the statement for odd n, add a Hopf-linked unknot to the above diagrams.

Now we prove (3). It is enough to prove that $A_{n,m}(G)$ and $D_{n,m}(G)$ are GPV finite type invariants, because any GPV finite type invariant is automatically of Kauffman finite type. But [10, page 12] implies, that any invariant given by an arrow diagram formula with n arrows is GPV finite type of degree n. □

Remark 3.8. It follows from [6, Theorem 1.1], that (2) in Theorem 3.7 follows from (3).

Let K_T be a virtual knot with a virtual diagram shown in Figure 12. This knot is called the Kishino knot. It has attracted attention for its remarkable property that it is a connected sum of two diagrams of the trivial knot; it has trivial Jones polynomial, $Z'_{K_T}(t, y) = 0$ (for the definition of Z' and its properties see [22] and Paragraph 3.4), and the virtual knot group of K_T is isomorphic to $\mathbb{Z}$, see [13]. It was first proved to be non-classical in [13]. We show that K_T is non-classical using the polynomials ∇_{asc}, ∇_{des} and $\nabla_{asc-des}$.

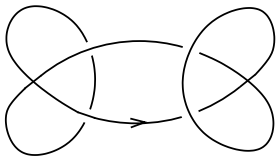

FIGURE 12. A diagram of the Kishino knot.

Proposition 3.9. *Polynomials ∇_{asc}, ∇_{des} and $\nabla_{asc-des}$ detect the fact that K_T is a non-classical knot.*

Proof. Recall that for any Gauss diagram G of a classical knot all these polynomials are independent of the position of the base point. Consider two Gauss diagrams G and $\widehat{G}$ of K_T which differ only by the position of the base point, see Figure 13.

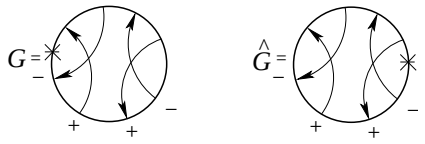

FIGURE 13. Gauss diagrams of the Kishino knot.

We have

$$\nabla_{asc}(G) = 1 - 2z^2 + z^4 \quad \nabla_{des}(G) = 1 \quad \nabla_{asc-des}(G) = -2z^2 + z^4 \quad \text{but}$$
$$\nabla_{asc}(\widehat{G}) = 1 \quad \nabla_{des}(\widehat{G}) = 1 - 2z^2 + z^4 \quad \nabla_{asc-des}(\widehat{G}) = 2z^2 - z^4.$$

□

Remark 3.10. In order to prove Proposition 3.9, i.e. to prove that the Kishino knot is not classical, it is enough to use Corollary 3.5, i.e. to show that $\nabla_{asc-des}(G) \neq 0$, where G is a Gauss diagram shown in Figure 13.

3.4. **Comparison with other constructions of Alexander-Conway polynomials of virtual links.** In [22] Sawollek associated to every link diagram D of a virtual link L a Laurent polynomial $Z'_D(t, y)$ in two variables t, y. He proved that $Z'_D(t, y)$ is an invariant of virtual links up to multiplication by powers of $t^{\pm 1}$, and that it vanishes on classical links. He also showed that $Z'_D(t, y)$ satisfies the following skein relation:

$$Z'_{D_+}(t, y) - Z'_{D_-}(t, y) = (t^{-1} - t)Z'_{D_0}(t, y),$$

where D_+, D_-, D_0 is a Conway triple of diagrams shown in Figure 21. It is obvious that both $\nabla_{asc}(L)$ and $\nabla_{des}(L)$ are crucially different from $Z'_L(t, y)$ because both of them do not vanish on classical links, but one can suspect that $\nabla_{asc-des}(L)$ coincides with $Z'_L(t, y)$ after a possible renormalization and a change of variables $z = t^{-1} - t$. Sawollek proved the following theorem:

Theorem 3.11 ([22])**.** *Let D, D_1, D_2 be virtual link diagrams and let $D_1 \sqcup D_2$ denote the disconnected sum of the diagrams D_1 and D_2. Then*

$$Z'_{D_1 \sqcup D_2}(t, y) = Z'_{D_1}(t, y)Z'_{D_2}(t, y).$$

Note that $\nabla_{asc-des}(L \sqcup L) = 0$ for any long virtual link L, but $Z'_{L \sqcup L}(t,y) = (Z'_L(t,y))^2$. Thus $\nabla_{asc-des}(L)$ is also different from $Z'_L(t,y)$.

Other generalizations of Alexander polynomials to virtual links are derived from the virtual and extended virtual link groups, see [22] and [23, 24] respectively.

1. Following [22] we denote by $\Delta_L(t)$ a polynomial which is derived from the virtual link group of a link L. It is well defined up to sign and multiplication by powers of $t^{\pm 1}$. For every virtual link diagram D the associated polynomial is denoted by $\Delta_D(t)$. In contrast to the classical Alexander polynomial, the Alexander polynomial of [22] for virtual links does not satisfy any linear skein relation as stated in the next theorem:

Theorem 3.12 ([22])**.** *For any normalization $A_D(t)$ of the polynomial $\Delta_D(t)$, i.e., $A_D(t) = \varepsilon_D t^{n_D} \Delta_D(t)$ with some $\varepsilon_D \in \{-1, 1\}$ and $n_D \in \mathbb{Z}$, the equation $p_1(t)A_{D_+}(t) + p_2(t)A_{D_-}(t) + p_3(t)A_{D_0}(t) = 0$ with $p_1(t), p_2(t), p_3(t) \in \mathbb{Z}[t^{\pm 1}]$ has only the trivial solution $p_1(t) = p_2(t) = p_3(t) = 0$.*

Since ∇_{asc}, ∇_{des} and $\nabla_{asc-des}$ satisfy the Conway skein relation, it follows that all of them are different from $\Delta_D(t)$ of [22].

2. Let L be a virtual link. The polynomial $\Delta_1(L)$ of [23, 24] is a polynomial in variables v, u and is well defined up to multiplication by powers of $(uv)^{\pm 1}$. If L is a classical link, then $\Delta_1(L)$ is equal to the Alexander polynomial in the variable uv. It follows that $\nabla_{asc-des}$ is different from Δ_1, because Δ_1 is not identically zero on the family of classical links.

Given a virtual link L, we denote by L^* the mirror image of L, i.e. a link obtained by inverting the sign of each classical crossing in a diagram of L. The following corollary was proved in [24].

Corollary 3.13 ([24], Corollary 5.2)**.** *Let L be a virtual m-component link. Then*

$$\Delta_1(L)(u,v) = (-1)^m \Delta_1(L^*)(v,u)$$

up to multiplication by powers of $(uv)^{\pm 1}$.

In particular, for any virtual knot $\Delta_1(K)(u,v) = -\Delta_1(K^*)(v,u)$.

Consider a mirror pair of long virtual knots K and K^* with Gauss diagrams G and G^* shown in Figure 14.

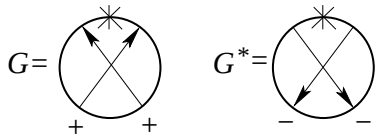

FIGURE 14. A mirror pair of Gauss diagrams.

Then $\nabla_{asc}(K) = \nabla_{des}(K^*) = 1 + z^2$, $\nabla_{asc}(K^*) = \nabla_{des}(K) = 1$. Thus both ∇_{asc} and ∇_{des} are different from $\Delta_1(L)$ in [23, 24].

Another way to see that both ∇_{asc} and ∇_{des} are different from Δ_1 is by finding a virtual knot K, such that both ∇_{asc} and ∇_{des} detect that this knot is non-classical, but $\Delta_1(K) = 1$ (so Δ_1 does not distinguish this knot from the unknot). An example

of such a knot K, together with a pair G and $\widehat{G}$ of its Gauss diagrams which differ by the position of the base point, is given in Figure 15. It was shown in [24] that $\Delta_1(K) = 1$.

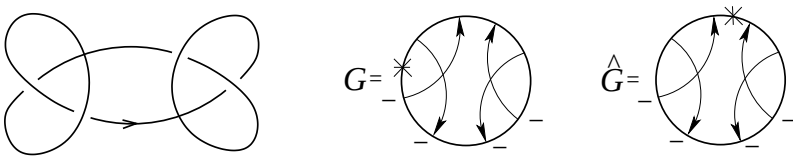

FIGURE 15. A virtual knot and two of its based Gauss diagrams.

We have

$$\nabla_{asc}(G) = 1 + z^2 \qquad \nabla_{des}(G) = 1 + z^2 \qquad \text{but}$$
$$\nabla_{asc}(\widehat{G}) = 1 + 2z^2 + z^4 \qquad \nabla_{des}(\widehat{G}) = 1.$$

It follows that both ∇_{asc} and ∇_{des} show that K is non-classical.

Finally, another generalization of the Alexander polynomial (related to the polynomial Z' of [22]) to long virtual knots was presented in [1]. It is a Laurent polynomial ζ in a variable t over the following ring $T = \mathbb{Z}[p, p^{-1}, q, q^{-1}]/((p-1)(p-q), (q-1)(p-q))$. This polynomial also vanishes on classical knots and thus ζ significantly differs from ∇_{asc} and ∇_{des}.

Question. Is it possible to derive $\nabla_{asc-des}$ from ζ?

4. Counting surfaces with two boundary components

In this section we present a new infinite family of Gauss diagram formulas, which correspond to counting of orientable surfaces with two boundary components. At the end of this section we identify the resulting invariants with certain derivatives of the HOMFLYPT polynomial.

4.1. **Link invariants and diagrams with two boundary components.**

In this subsection we define invariants of classical links using ascending and descending arrow diagrams with two boundary components.

Recall that for every Gauss diagram G we defined notions of ascending and descending separating states of G, see Subsection 2.5. Also, for every ascending (respectively descending) separating state S of G and for an arrow diagram $A \in \mathcal{A}^2_{n,m}$ (respectively $A \in \mathcal{D}^2_{n,m}$) we defined, in the same subsection, a notion of S-admissible pairing $\langle A, G\rangle_S$. Note that every ascending (respectively descending) separating state S of G defines two Gauss diagrams G'_S and G''_S as follows: G'_S (respectively G''_S) consists of all circles of G_S labeled by 1 (respectively by 2), and its arrows are arrows of G with both ends on these circles. All arrows with ends on circles of G_S with different labels are removed. The base point on G'_S is the base point $*$ of G. The base point on G''_S is placed near the first arrow in S which we encounter as we walk on G starting from $*$.

If G is a Gauss diagram of a classical link L, then G'_S and G''_S correspond to classical links L'_S and L''_S, which are defined as follows. We smooth all crossings which correspond to arrows in S, as shown below:

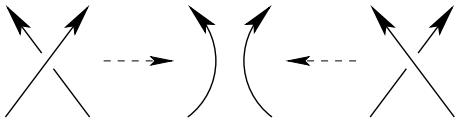

We obtain a diagram of a smoothed link L_S with labeling of components induced from the labeling of circles of G_S. Denote by L'_S and L''_S sublinks which consist of components labeled by 1 and 2 respectively. Let m' and m'' denote the number of components of L'_S and L''_S respectively, and as usual let G'_S, G''_S be the corresponding Gauss diagrams. It is an immediate consequence of Definition 2.19 that

$$A^2_{n,m}(G)_S = \text{sign}(S) \sum_{i=0}^{n-|S|} A_{i,m'}(G'_S) A_{n-|S|-i,m'}(G''_S)$$

$$D^2_{n,m}(G)_S = \text{sign}(S) \sum_{i=0}^{n-|S|} D_{i,m'}(G'_S) D_{n-|S|-i,m'}(G''_S),$$

where $|S|$ is the number of arrows in S and $\text{sign}(S) = \prod_{\alpha \in S} \text{sign}(\alpha)$.

It follows from Corollary 3.5 that for every $n \geq 0$ we have

$$A_{n,m'}(G'_S) = D_{n,m'}(G'_S) = c_n(L'_S) \quad \text{and} \quad A_{n,m''}(G''_S) = D_{n,m''}(G''_S) = c_n(L''_S)$$

. As an immediate corollary we get

Lemma 4.1. *Let G be a Gauss diagram of an m-component link L. Then for every $n \geq 0$ and an ascending (respectively descending) separating state S of G we have*

$$A^2_{n,m}(G)_S = \text{sign}(S) \sum_{i=0}^{n-|S|} c_i(L'_S) c_{n-|S|-i}(L''_S)$$

$$D^2_{n,m}(G)_S = \text{sign}(S) \sum_{i=0}^{n-|S|} c_i(L'_S) c_{n-|S|-i}(L''_S).$$

Summing over all ascending (descending) separating states S, we obtain

Corollary 4.2. *Let G be any Gauss diagram of an m-component link L. Then for every $n \geq 0$ we have*

$$A^2_{n,m}(G) = \sum_{k=1}^{n} \sum_{S,|S|=k} \text{sign}(S) \sum_{i=0}^{n-k} c_i(L'_S) c_{n-k-i}(L''_S)$$

$$D^2_{n,m}(G) = \sum_{k=1}^{n} \sum_{S,|S|=k} \text{sign}(S) \sum_{i=0}^{n-k} c_i(L'_S) c_{n-k-i}(L''_S)$$

where the second summation is over all ascending and descending separating states S of G respectively.

It turns out that both $A^2_{n,m}(G)$ and $D^2_{n,m}(G)$ are invariant under Ω_2 and Ω_3:

Theorem 4.3. *Let G be any Gauss diagram of an m-component link L. Then $A^2_{n,m}(G)$ and $D^2_{n,m}(G)$ are invariant under Reidemeister moves Ω_2 and Ω_3 which do not involve the base point.*

Proof. We will prove the invariance of $A^2_{n,m}(G)$; the proof for $D^2_{n,m}(G)$ is the same.

Let G and $\widetilde{G}$ be two Gauss diagrams that differ by an application of Ω_2, so that $\widetilde{G}$ has two additional arrows α_ε and $\alpha_{-\varepsilon}$, see Figure 3. Ascending states of G are in bijective correspondence with ascending states of $\widetilde{G}$ which do not contain $\alpha_{\pm\varepsilon}$. Note that α_ε and $\alpha_{-\varepsilon}$ can not be both in the image of $\phi : A \to G$ with $A \in \mathcal{A}^2_{n,m}$, because A is an ascending diagram with two boundary components. Ascending states of $\widetilde{G}$ which contain one of $\alpha_{\pm\varepsilon}$ come in pairs $S \cup \alpha_\varepsilon$ and $S \cup \alpha_{-\varepsilon}$ with opposite signs, thus cancel out in $A^2_{n,m}(\widetilde{G})$. Hence

$$A^2_{n,m}(G) = A^2_{n,m}(\widetilde{G}).$$

Now, let G and $\widetilde{G}$ be two Gauss diagrams that differ by an application of Ω_3, see Figure 3 (G is on the left and $\widetilde{G}$ is on the right). Denote the top, left, and right arrows in the fragment by α_t, α_l, and α_r respectively. There is a bijective correspondence between ascending separating states of G and $\widetilde{G}$, such that none of the arrows α_r, α_l and α_t belong to these states. Indeed, we may identify separating states of G and $\widetilde{G}$ which have the same arrows and the same labeling of arcs. For any such separating state S we have $A^2_{n,m}(G)_S = A^2_{n,m}(\widetilde{G})_S$ by Lemma 4.1 and Theorem 3.2.

An ascending separating state of G or $\widetilde{G}$ may contain either exactly one arrow of the fragment i.e. α_r or α_l or α_t, or it may contain both arrows α_r and α_l. There is a bijective correspondence between ascending separating states of G and $\widetilde{G}$ which contain α_l. Two possible cases of this correspondence (which differ by the labeling) are shown in Figure 16 and Figure 17. Abusing the notation we denote the corresponding ascending separating states by S_r, S_l, S_t, S_{lr}, and $\widetilde{S}_r$, $\widetilde{S}_l$, $\widetilde{S}_t$, $\widetilde{S}_{lr}$.

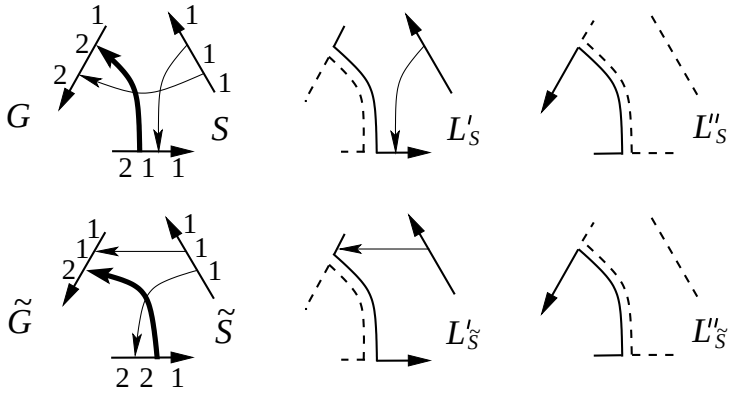

FIGURE 16. Identifying ascending separating states containing α_l.

In both cases, links L'_S and L''_S constructed from G and $\widetilde{G}$ are isotopic, thus by Lemma 4.1 $A^2_{n,m}(G)_S = A^2_{n,m}(\widetilde{G})_{\widetilde{S}}$. The situation with ascending separating states which contain α_r is completely similar and is omitted.

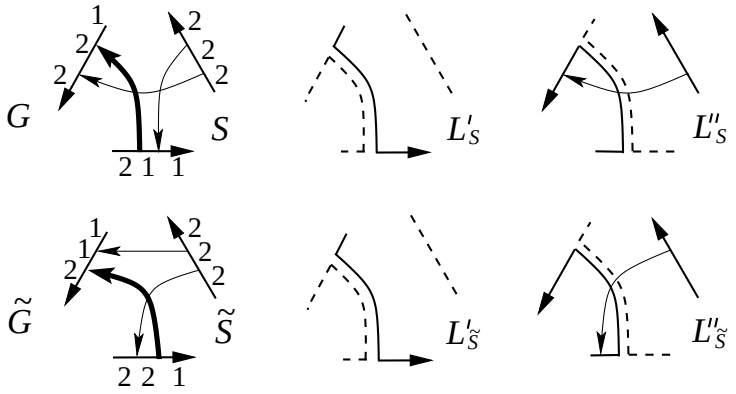

FIGURE 17. Identifying other ascending separating states containing α_l.

The correspondence of ascending separating states which contain $\alpha_l \cup \alpha_r$ or α_t is more complicated. One of the two possible cases is summarized in Figure 18.

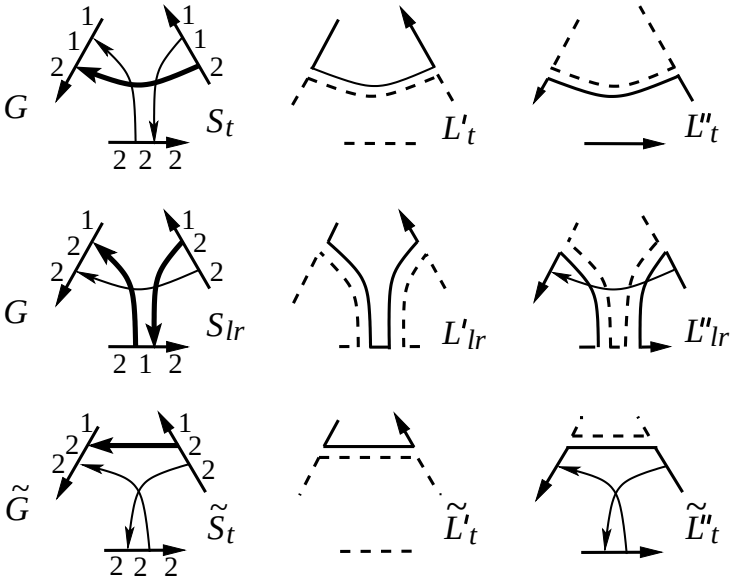

FIGURE 18. Comparison of ascending separating states of G and $\widetilde{G}$.

Links $\widetilde{L'}_t$, L'_t and L'_{lr} are isotopic, thus

$$c_i(\widetilde{L'}_t) = c_i(L'_t) = c_i(L'_{lr}).$$

For $c_i(\widetilde{L}''_t)$ we have:

$$c_i\left(\begin{array}{c}\includegraphics[height=1.2em]{}\end{array}\right) = c_i\left(\begin{array}{c}\includegraphics[height=1.2em]{}\end{array}\right) + c_{i-1}\left(\begin{array}{c}\includegraphics[height=1.2em]{}\end{array}\right) = c_i\left(\begin{array}{c}\includegraphics[height=1.2em]{}\end{array}\right) + c_{i-1}\left(\begin{array}{c}\includegraphics[height=1.2em]{}\end{array}\right).$$

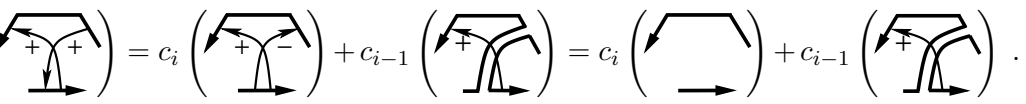

The first equality is the skein relation of Theorem 3.3, and the second equality holds by the invariance of c_i under Ω_2. Hence

$$c_i(\widetilde{L}''_t) = c_i(L''_t) + c_{i-1}(L''_{lr}).$$

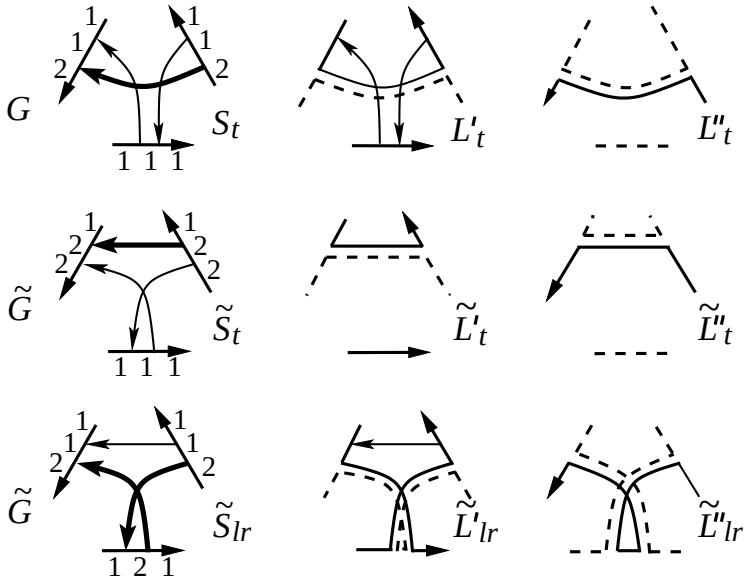

FIGURE 19. Comparison of other ascending separating states of G and $\widetilde{G}$.

Denote by k the number of arrows in S_t, where S_t is shown in Figure 18. Note that the number of arrows in $\widetilde{S}_t$ and S_{lr} is k and $k+1$, respectively. Thus

$$\sum_{i=0}^{n-k} c_i(\widetilde{L}'_t)c_{n-k-i}(\widetilde{L}''_t) = \sum_{i=0}^{n-k} c_i(L'_t)c_{n-k-i}(L''_t) + \sum_{i=0}^{n-k-1} c_i(L'_{lr})c_{n-k-i-1}(L''_{lr}).$$

Note that $\operatorname{sign}(\widetilde{S}_t) = \operatorname{sign}(S_t) = \operatorname{sign}(S_{lr})$, thus by Lemma 4.1

$$A^2_{n,m}(\widetilde{G})_{\widetilde{S}_t} = A^2_{n,m}(G)_{S_t} + A^2_{n,m}(G)_{S_{lr}}.$$

The second possible case (which differs by labeling) is shown in Figure 19. Abusing the notation we again denote the corresponding ascending separating states by S_t, $\widetilde{S}_t$, $\widetilde{S}_{lr}$. Links L''_t, $\widetilde{L}''_t$ and $\widetilde{L}''_{lr}$ are isotopic. Applying the skein relation for $c_i(L'_t)$ similarly to the above, in this case we get

$$A^2_{n,m}(G)_{S_t} = A^2_{n,m}(\widetilde{G})_{\widetilde{S}_t} + A^2_{n,m}(\widetilde{G})_{\widetilde{S}_{lr}}.$$

□

Our next step is to study the behavior of $A^2_{n,m}(G)$ and $D^2_{n,m}(G)$ under an application of the move Ω_1. Both $A^2_{n,m}(G)$ and $D^2_{n,m}(G)$ change under Ω_1, see Example 4.4.

Example 4.4. Let G, G_1 and G_2 be Gauss diagrams of an unknot shown in Figures 20a, 20b and 20c respectively. Then $D^2_{1,1}(G) = 0$, but $D^2_{1,1}(G_1) = 1$; and $A^2_{1,1}(G) = 0$, but $A^2_{1,1}(G_2) = -1$.

However, this problem is easy to solve. Denote by

$$AD_{n,m}(G) := A^2_{n,m}(G) + D^2_{n,m}(G)$$

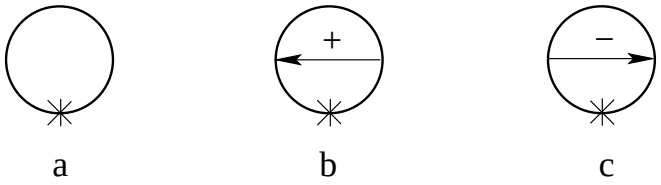

FIGURE 20. Gauss diagrams G, G_1 and G_2.

and let

$$I_{n,m}(G) := AD_{n,m}(G) - w(G)c_{n-1}(L),$$

where $w(G)$ is the writhe of G, i.e. the sum of signs of all arrows in G.

Theorem 4.5. *Let G be a Gauss diagram of a long m-component link L. Then $I_{n,m}(G)$ is an invariant of an underlying link L, i.e. is independent of a choice of G.*

Proof. By Theorem 4.3, it remains to prove the invariance of $I_{n,m}$ under Ω_1 (applied away from the base point). Let $\widetilde{G}$ and G be two Gauss diagrams which are related by an application of Ω_1, such that $\widetilde{G}$ contains a new isolated arrow α. Then α contributes either a new ascending or a new descending separating state $\{a\}$, depending on whether we meet its head or tail first on the passage from the base point. Contribution of this state to $AD_{n,m}(\widetilde{G})$ is either $\mathrm{sign}(\alpha)A_{n-1,m}(G)$, or $\mathrm{sign}(\alpha)D_{n-1,m}(G)$; but

$$\mathrm{sign}(\alpha)A_{n-1,m}(G) = \mathrm{sign}(\alpha)c_{n-1}(L) = \mathrm{sign}(\alpha)D_{n-1,m}(G)$$

by Corollary 3.5, thus

$$I_{n,m}(\widetilde{G}) - I_{n,m}(G) = (\mathrm{sign}(\alpha) - w(\widetilde{G}) + w(G))c_{n-1}(L).$$

It remains to note that $w(\widetilde{G}) - w(G) = \mathrm{sign}(\alpha)$. □

Our next step is to study dependence of $A^2_{n,m}(G)$ and $D^2_{n,m}(G)$ on the position of the base point. The example below shows that each of them depends on the base point.

Example 4.6. Let G and $\widehat{G}$ be two Gauss diagrams of the right-handed trefoil shown below. Then $A^2_{3,1}(G) = 0$ and $D^2_{3,1}(G) = 1$, but $A^2_{3,1}(\widehat{G}) = 1$ and $D^2_{3,1}(\widehat{G}) = 0$.

However, it turns out that the sum $A^2_{n,m}(G)+D^2_{n,m}(G) = AD_{n,m}(G)$ does not depend on the base point. Indeed, let G and $\widehat{G}$ be two Gauss diagrams which differ only by a position of their base points. Let $\widehat{S}$ be an ascending separating state of $\widehat{G}$. If an arc which contains the base point $*$ of G is labeled by 1, then $S = \widehat{S}$ is an ascending separating state of G and by Lemma 4.1 we have $A^2_{n,m}(G)_S = A^2_{n,m}(\widehat{G})_{\widehat{S}}$. If an arc which contains the base point $*$ of G is labeled by 2, we consider a descending separating state S of G which has the same arrows as $\widehat{S}$, but opposite labels. By Lemma 4.1, $D^2_{n,m}(G)_S = A^2_{n,m}(\widehat{G})_{\widehat{S}}$. We repeat this process, replacing ascending separating states with descending and A with D. Summing up by separating states, in view of Corollary 4.2 we obtain the following

Theorem 4.7. *Let G be a based Gauss diagram of an m-component link L. Then $AD_{n,m}(G)$ is independent of the position of the base point.*

Note that $AD_{n,m}(G)$ is invariant under Ω_1^F move. Now Theorems 4.3 and 4.7 imply two important corollaries.

Corollary 4.8. *Let G be any Gauss diagram of an m-component framed link L. Then $AD_n(L) = AD_{n,m}(G)$ is an invariant of an underlying framed link, i.e does not depend on G.*

Corollary 4.9. *Let G be any Gauss diagram of an m-component link L. Then $I_n(L) := I_{n,m}(G)$ is an invariant of an underlying link L, i.e. is independent of a choice of G.*

5. Properties of I_n

In this section we establish the skein relation for $I_{n,m}$. Then we identify $I_{n,m}$ with coefficients of a certain polynomial, which is derived from the HOMFLYPT polynomial.

5.1. **Skein relation.** In this part we establish the skein relation for $AD_{n,m}(G)$. First we recall a notion of the Conway triple of links.

Let L_+, L_- and L_0 be a triple of links with diagrams which are identical except for a small fragment, where L_+ and L_- have a positive and a negative crossing respectively, and L_0 has a smoothed crossing, see Figure 21. Such a triple of links is called a *Conway triple*.

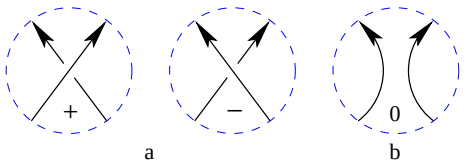

Figure 21. Conway triple

Theorem 5.1. *Let L_+, L_-, L_0 be a Conway triple of links with the corresponding Conway triple G_+, G_-, G_0 of Gauss diagrams, see Figures 21 and 8. Denote the number of circles of $G_\pm$ and G_0 by m and m_0, respectively. Then*

$$AD_{n,m}(G_+) - AD_{n,m}(G_-) = \begin{cases} AD_{n-1,m_0}(G_0)\ , & \text{if } m_0 = m-1 \\ AD_{n-1,m_0}(G_0) + \sum\limits_{L' \subset L_0} \sum\limits_{i=0}^{n-1} c_i(L') c_{n-i-1}(L_0 \smallsetminus L') & \text{if } m_0 = m+1, \end{cases} \tag{6}$$

where the summation is over all sublinks L' of L_0 which contain exactly one of the two new sublinks resulting from the smoothing.

Proof. Denote the arrows of G_+ and G_- appearing in Figure 8 by α_+ and α_-, respectively. Let us look at labels of ascending separating states of $G_\pm$ and G_0 on four arcs of the shown fragment. If labels of all four arcs are the same, we may identify states of $G_\pm$ and G_0 with the same arrows and labels of arcs, see Figure 22a. Lemma 4.1 and Conway skein relation imply, that for every such state S

$$A^2_{n,m}(G_+)_S - A^2_{n,m}(G_-)_S = A^2_{n-1,m_0}(G_0)_S.$$

The descending case is treated similarly.

If labels on two arcs near the head of $\alpha_\pm$ coincide, but differ from labels near the tail of $\alpha_\pm$, by Lemma 4.1 we have $A^2_{n,m}(G_+)_S - A^2_{n,m}(G_-)_S = 0$ for any such state S of $G_\pm$, and there is no corresponding state of G_0, see Figure 22b. The descending case is treated similarly.

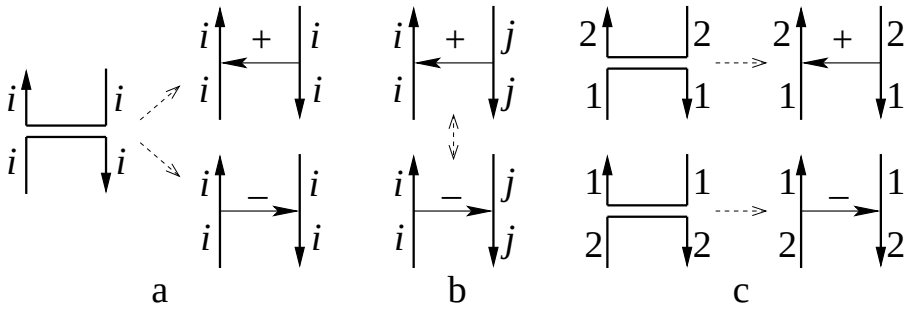

FIGURE 22. Correspondence of separating states of G_0 and $G_\pm$.

There are two further cases when labels of two arcs near the head of $\alpha_\pm$ are different. Such a state S of G_0 corresponds either to an ascending separating state $S \cup \alpha_+$ of G_+, or to an ascending separating state $S \cup \alpha_-$ of G_-, see Figure 22c. By Lemma 4.1 we have $A^2_{n,m}(G_+)_{S\cup\alpha_+} = A^2_{n-1,m_0}(G_0)_S$ in the first case and $A^2_{n,m}(G_-)_{S\cup\alpha_-} = -A^2_{n-1,m_0}(G_0)_S$ in the second case.

If $m_0 = m-1$, there are no other ascending separating states of any of the diagrams and, repeating this computation for descending separating states, summing over states and using Corollary 4.2, we obtain the first equality in (6).

If $m_0 = m+1$, both ends of $\alpha_\pm$ are on the same circle of $G_\pm$ and there is an additional contribution to $AD_{n,m}(G_\pm)$ of separating states $S = \{\alpha_\pm\}$ of $G_\pm$, which contain only the arrow $\alpha_\pm$ (and some labeling of arcs)[1]. Such separating states correspond to labeling all circles of G_0 by 1, 2 so that the based circle is labeled by 1, and two new components of G_0 resulting from the smoothing have different labels. Denote by L' the sublink labeled by 1. The case of descending separating states $\{\alpha_\pm\}$ is similar. By Corollary 4.2, the contribution of these states to $AD_{n,m}(G_+) - AD_{n,m}(G_-)$ equals

$$\sum_{L'\subset L_0} \sum_{i=0}^{n-1} c_i(L')c_{n-i-1}(L_0 \smallsetminus L')$$

and the proof follows. □

[1]These states have no counterpart in G_0, since such a separating state of G_0 should be empty and corresponding surface disconnected.

5.2. **Identification of the invariant I_n.** In this subsubsection we identify I_n with certain derivatives of the HOMFLYPT polynomial.

Let $P(L)$ be the HOMFLYPT polynomial of a link L. We denote by $P'_a(L)$ the first derivative of $P(L)$ w.r.t. a. Then $P'_a(L)|_{a=1}$ is a polynomial in the variable z. We denote by $p_n(L)$ the coefficient of z^n in $zP'_a(L)|_{a=1}$. Note that $p_n(L)$ a finite type invariant of degree n, see [11], and hence by the Goussarov theorem it admits a Gauss diagram formula involving arrow diagrams with up to n arrows. The precise formula is shown in the next theorem.

Theorem 5.2. *Let L be an m-component link. Then for every $n \geq 0$*

$$I_n(L) = p_n(L) - C_n(L), \tag{7}$$

where $C_n(L)$ is defined by

$$C_n(L) := \sum_{L' \subset L} \sum_{i=0}^{n} c_i(L') c_{n-i}(L \smallsetminus L'),$$

and the summation is over all proper sublinks L' of L.

Proof. It is enough to show that $I_n(L) + C_n(L)$ and $p_n(L)$ satisfy the same skein relation and take the same value on unlinks with any number of components.

The skein relation for $zP'_a(L)|_{a=1}$ follows directly from the skein relation for $P(L)$, see (1). Differentiating this skein relation w.r.t. a, substituting $a = 1$, and multiplying by z we obtain

$$zP'_a(L_+)|_{a=1} - zP'_a(L_-)|_{a=1} + zP(L_+)|_{a=1} + zP(L_-)|_{a=1} = z^2 P'_a(L_0)|_{a=1}.$$

Note that $P(L)|_{a=1} = \nabla(L)$ is the Conway polynomial of L. Thus

$$zP'_a(L_+)|_{a=1} - zP'_a(L_-)|_{a=1} + z\nabla(L_+) + z\nabla(L_-) = z^2 P'_a(L_0)|_{a=1}.$$

Taking the n-th coefficient, we get

$$p_n(L_+) - p_n(L_-) + c_{n-1}(L_+) + c_{n-1}(L_-) = p_{n-1}(L_0). \tag{8}$$

The skein relation for C_n is obtained directly from the Conway skein relation. It depends on the number m_0 of the components in L_0:

$$C_n(L_+) - C_n(L_-) = \begin{cases} C_{n-1}(L_0), \text{ if } m_0 = m - 1 \\ 2 \sum\limits_{L' \subset L_0} \sum\limits_{i=0}^{n-1} c_i(L') c_{n-i-1}(L_0 \smallsetminus L') \text{ if } m_0 = m + 1, \end{cases} \tag{9}$$

where the summation is over all sublinks L' of L_0 which contain both new components appearing after the smoothing. Now Theorem 5.1 and equality (9) yield

$$AD_{n,m}(G_+) - AD_{n,m}(G_-) + C_n(L_+) - C_n(L_-) = AD_{n-1,m_0}(G_0) + C_{n-1}(L_0).$$

Deducting $w(G_0)c_{n-2}(L_0)$ from both sides of this equation and noticing that $w(G_0) = w(G_+) - 1 = w(G_-) + 1$ and $c_{n-1}(L_+) - c_{n-1}(L_-) = c_{n-2}(L_0)$, so

$$w(G_0)c_{n-2}(L_0) = w(G_+)c_{n-1}(L_+) - w(G_+)c_{n-1}(L_+) - c_{n-1}(L_+) - c_{n-1}(L_-),$$

we obtain the desired skein relation for $I_n(L) + C_n(L)$:

$$(I_n(L_+) + C_n(L_+)) - (I_n(L_-) + C_n(L_-)) + c_{n-1}(L_+) + c_{n-1}(L_-) = I_{n-1}(L_0) + C_{n-1}(L_0).$$

It remains to compare values of $I_n(L) + C_n(L)$ and $p_n(L)$ on an m-component unlink O_m. From the definition of $I_n(L)$ we get $I_n(O_m) = AD_{n,m}(O_m) = 0$ for any n and m. Also, the equality $p_n(O_m) = C_n(O_m)$ holds for any n and m, since $p_0(O_2) = C_0(O_2) = 2$ and $p_n(O_m) = C_n(O_m) = 0$ otherwise. This concludes the proof of the theorem. □

Example 5.3. Let G be a Gauss diagram of a link H_2 shown in Figure 23.

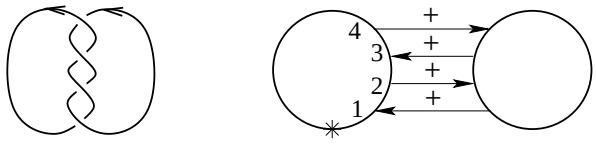

FIGURE 23. Link H_2 and its Gauss diagram.

Let us calculate $C_n(H_2)$ and $I_n(H_2)$. Both components of H_2 are trivial, so $C_0(H_2) = 2$ and $C_n(H_2) = 0$ for $n \neq 0$. The only ascending states of G are $\{1,2\}$, $\{1,4\}$, and $\{3,4\}$; the only descending state of G is $\{2,3\}$. Thus $AD_{2,2}(G) = 4$. Note that $c_1(H_2) = 2$ and $c_n(H_2) = 0$ for $n \neq 1$, thus $I_2(H_2) = 4 - 4 \cdot 2 = -4$ and $I_n(H_2) = 0$ for $n \neq 2$. Indeed, one may check that $P(H_2) = a^{-3}z^{-1} - a^{-5}z^{-1} + a^{-3}z + a^{-1}z$, so $zP'_a(H_2)|_{a=1} = 2 - 4z^2$.

6. Last Remarks

6.1. **The case of knots.** In this subsection we define for every $n \geq 0$ another two invariants $I_{A,n}$ and $I_{D,n}$ of classical knots.

Definition 6.1. Let G be a based Gauss diagram of a knot K. We go on the circle of G starting from the base point until we return to the base point. Denote by $w_A(G)$ (respectively $w_D(G)$) sum of signs of all arrows of G which we pass first at the arrowhead (respectively arrowtail).

Theorem 6.2. *Let G be any based Gauss diagram of a knot K. Then for every $n \geq 0$ both*

$$I_{A,n}(G) := A^2_{n,1}(G) - w_A(G) \cdot c_{n-1}(K),$$
$$I_{D,n}(G) := D^2_{n,1}(G) - w_D(G) \cdot c_{n-1}(K)$$

are invariants of a knot K.

These invariants will be denoted by $I_{A,n}(K)$ and $I_{D,n}(K)$ respectively.

Proof. We will prove the invariance of $I_{A,n}(G)$; the proof for $I_{D,n}(G)$ is the same.

A well-known fact in knot theory is that for classical knots, theories of closed and long knots are equivalent. Thus it suffices to prove the invariance of $I_{A,n}(G)$ under Reidemeister moves $\Omega_1 - \Omega_3$ applied away from the base point. Note that both $w_A(G)$ and $A^2_{n,1}(G)$ are invariant under Ω_2 and Ω_3 (see Lemma 4.3). It remains to prove the invariance of $I_{A,n}(G)$ under Ω_1. Let G and $\widetilde{G}$ be two based Gauss diagrams that differ by an application of Ω_1, so that $\widetilde{G}$ has an additional isolated arrow α either as in Figure 24a, or as in Figure 24b.

FIGURE 24. Two versions of the Reidemeister move Ω_1.

In the first case, $A^2_{n,1}(\widetilde{G}) = A^2_{n,1}(G)$ and $w_A(\widetilde{G}) = w_A(G)$, thus we have $I_{A,n}(G) = I_{A,n}(\widetilde{G})$. In the second case, by Corollary 3.5 we get

$$A^2_{n,1}(\widetilde{G}) = A^2_{n,1}(G) + \varepsilon c_{n-1}(K).$$

We also have $w_A(\widetilde{G}) = w_A(G) + \varepsilon$, and thus again $I_{A,n}(G) = I_{A,n}(\widetilde{G})$. □

Note that for every G we have $w(G) = w_A(G) + w_D(G)$; also, for knots one has $I_n(K) = p_n(K)$.

Corollary 6.3. *For every knot K we have $I_n(K) = I_{A,n}(K) + I_{D,n}(K) = p_n(K)$.*

6.2. **Irreducible arrow diagrams.** In this subsection we define a modification of link invariants considered in Section 3. This modification allows us to reduce significantly the number of diagrams in formulas for link invariants by using a special type of arrow diagrams – so called irreducible diagrams.

Definition 6.4. An arrow diagram A is called *irreducible* if after the removal of any arrow in A the remaining graph is connected. Otherwise, A is called *reducible*.

Example 6.5. Irreducible diagrams in $\mathcal{A}_{3,2}$ are shown in Figure 25a, and reducible diagrams are shown in Figure 25b.

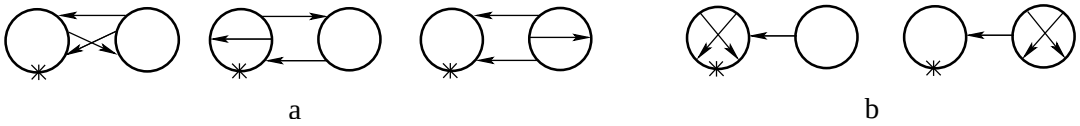

FIGURE 25.

Denote by $\mathcal{AI}r_{n,m} \subset \mathcal{A}_{n,m}$ sets of all irreducible ascending diagrams with m circles, n arrows, and one boundary component. Descending diagrams of the same types we

will denote using $\mathcal{D}$ instead of $\mathcal{A}$. Let G be a Gauss diagram of an m-component link L. Define $\mathcal{AI}r_{n,m}(G)$ and $\mathcal{DI}r_{n,m}(G)$ by

$$\mathcal{AI}r_{n,m}(G) := \sum_{A\in\mathcal{AI}r_{n,m}} \langle A, G\rangle \qquad \mathcal{DI}r_{n,m}(G) := \sum_{A\in\mathcal{DI}r_{n,m}} \langle A, G\rangle.$$

Theorem 6.6. *Let G be a Gauss diagram of an m-component link L. Then both $\mathcal{AI}r_{n,m}(G)$ and $\mathcal{DI}r_{n,m}(G)$ are invariants of an underlying link L. Moreover,*

$$\mathcal{AI}r_{n,m}(G) = \mathcal{DI}r_{n,m}(G).$$

Proof. For the simplicity we prove this theorem in case of two-component links, i.e. $m = 2$. The proof for general m is very similar and is left to the reader.

Let G be any Gauss diagram of a two-component classical link $L = L_1 \cup L_2$, and let $A \in \mathcal{A}_{n,2}$ be an arrow diagram with exactly one arrow between two different circles. The set of such arrow diagrams is denoted by $\overleftarrow{\mathcal{A}}_{n,2}$. We denote the set of descending diagrams of the same type by $\overrightarrow{\mathcal{D}}_{n,2}$. We set

$$\overleftarrow{A}_{n,2}(G) := \sum_{A\in\overleftarrow{\mathcal{A}}_{n,2}} \langle A, G\rangle \qquad \overrightarrow{D}_{n,2}(G) := \sum_{A\in\overleftarrow{\mathcal{D}}_{n,2}} \langle A, G\rangle.$$

Now we prove that

$$\overleftarrow{A}_{n,2}(G) = \mathrm{lk}(L_1, L_2)\sum_{k=0}^{n-1} c_k(L_1)c_{n-k-1}(L_2) = \overrightarrow{D}_{n,2}(G). \tag{10}$$

We start with the case of ascending diagrams. Let G_1 and G_2 be diagrams obtained from G by erasing arrows between circles of G. We denote by $\mathfrak{A}(G)$ a set of arrows which are oriented from the non-based circle of G to the based one. Without loss of generality suppose that a base point $*$ of G lies on G_1. We pick $\alpha \in \mathfrak{A}(G)$ and erase all other arrows in $\mathfrak{A}(G)$. The remaining diagram is denoted by G_α. We place on G_2 a base point $*_\alpha$ at the tail of α. Then

$$\sum_{A\in\overleftarrow{\mathcal{A}}_{n,2}} \overleftarrow{A}_{n,2}(G_\alpha) = \mathrm{sign}(\alpha)\sum_{k=0}^{n-1} A_{k,2}(G_1)A_{n-k-1,2}(G_2) = \mathrm{sign}(\alpha)\sum_{k=0}^{n-1} c_k(L_1)c_{n-k-1}(L_2),$$

where the last equality is by Corollary 3.5. It follows that

$$\overleftarrow{A}_{n,2}(G) = \sum_{\alpha\in\mathfrak{A}(G)}\sum_{A\in\overleftarrow{\mathcal{A}}_{n,2}} \overleftarrow{A}_{n,2}(G_\alpha) = \mathrm{lk}(L_1, L_2)\sum_{k=0}^{n-1} c_k(L_1)c_{n-k-1}(L_2).$$

In case of descending diagrams, we denote by $\mathfrak{D}(G)$ a set of arrows which are oriented from the based circle of G to the non-based one. For $\alpha \in \mathfrak{D}(G)$ we place a base point $*_\alpha$ at the head of α. Now we proceed as in the former case and the proof of (10) follows. Note that by definition $\mathcal{AI}r_{n,2} = \mathcal{A}_{n,2} \setminus \overleftarrow{\mathcal{A}}_{n,2}$ and $\mathcal{DI}r_{n,2} = \mathcal{D}_{n,2} \setminus \overrightarrow{\mathcal{D}}_{n,2}$. Now the proof follows immediately from Corollary 3.5. □

References

[1] Afanasiev D.: *On a Generalization of the Alexander Polynomial for Long Virtual Knots,* Journal of Knot Theory and Its Ramifications Vol. 18, No. 10 (2009) 1329–1333.

[2] Brandenbursky M.: *Invariants of closed braids via counting surfaces,* Journal of Knot Theory and its Ramifications, vol. 22, No.3 (2013), 1350011 (21 pages).

[3] Chmutov S., Khoury M., Rossi A.: *Polyak-Viro formulas for coefficients of the Conway polynomial,* Journal of Knot Theory and Its Ramifications 18, no. 6 (2009), 773–783.

[4] Chmutov S., Duzhin S., Mostovoy J.: *Introduction to Vassiliev knot invariants,* to appear in Cambridge University Press, 2012.

[5] Chmutov S., Polyak M.: *Elementary combinatorics for HOMFLYPT polynomial,* Int. Math. Res. Notices (2009), doi:10.1093/imrn/rnp137.

[6] Chrisman M.: *On the Goussarov-Polyak-Viro finite-type invariants and the virtualization move,* Journal of Knot Theory and Its Ramifications Vol. 20, No. 3 (2011) 389–401.

[7] Conway J.: *An enumeration of knots and links,* Computational problems in abstract algebra, Ed.J.Leech, Pergamon Press, (1969), 329–358.

[8] Fiedler T.: *Gauss diagram invariants for knots and links,* Mathematics and Its Applications **532**, 2001.

[9] Freyd P., Yetter D., Hoste J., Lickorish W. B. R., Millett K., Ocneanu A.: *A new polynomial invariant of knots and links,* Bull. AMS 12 (1985), 239–246.

[10] Goussarov M., Polyak M., Viro O.: *Finite type invariants of classical and virtual knots,* Topology 39 (2000), 1045–1068.

[11] Kanenobu T., Miyazawa Y.: *HOMFLY polynomials as Vassiliev link invariants,* in Knot theory, Banach Center Publ. 42, Polish Acad. Sci., Warsaw (1998,) 165–185.

[12] Kauffman L.: *Virtual Knot Theory,* European J. Comb. Vol. 20 (1999), 663–690.

[13] Kishino T., Satoh S.: *A note on non-classical virtual knots*, Journal of Knot Theory and its Ramifications 13 no. 7 (2004), 845–856.

[14] Kravchenko O., Polyak M.: *Diassociative algebras and Milnor's invariants for tangles,* Letters Math. Physics 95 (2011), 297–316.

[15] Lickorish W. B. R.: *An Introduction to Knot Theory,* 1997 Springer-Verlag New York, Inc.

[16] Lickorish W. B. R., Millett K.: *A polynomial invariant of oriented links*, Topology 26 (1) (1987), 107–141.

[17] Matveev S., Polyak M.: *A simple formula for the Casson-Walker invariant*, Journal Knot Theory and its Ramifications 18 (2009), 841–864.

[18] Östlund O.-P.: *Invariants of knot diagrams and relations among Reidemeister moves,* Journal of Knot Theory and Its Ramifications 10, no. 8 (2001), 1215–1227.

[19] Polyak M.: *Minimal generating sets of Reidemeister moves,* Quantum Topology 1 (2010), 399–411.

[20] Polyak M., Viro O.: *Gauss diagram formulas for Vassiliev invariants*, Int. Math. Res. Notices 11 (1994), 445–454.

[21] Przytycki J., Traczyk P.: *Invariants of links of the Conway type*, Kobe J. Math. 4 (1988), 115–139.

[22] Sawollek J.: *On Alexander-Conway polynomials for virtual knots and links*, Journal of Knot Theory Ramifications 12, no. 6 (2003), 767–779.

[23] Silver D., Williams S.: *Alexander Groups and Virtual Links*, Journal of Knot Theory and Its Ramifications, 10 (2001), 151–160.

[24] Silver D., Williams S.: *Polynomial invariants of virtual links*, Journal of Knot Theory and its Ramifications 12 (2003), 987–1000.

Max-Planck-Institut für Mathematik, 53111 Bonn, Germany
E-mail address: brandem@mpim-bonn.mpg.de